B_s and D_s Decay Constants in Three-Flavor Lattice QCD

Matthew Wingate,[1,2] Christine T. H. Davies,[3] Alan Gray,[3,1] G. Peter Lepage,[4] and Junko Shigemitsu[1]

[1]*Department of Physics, The Ohio State University, Columbus, Ohio 43210, USA*
[2]*Institute for Nuclear Theory, University of Washington, Seattle, Washington 98195-1550, USA*
[3]*Department of Physics & Astronomy, University of Glasgow, Glasgow, G12 8QQ, United Kingdom*
[4]*Laboratory of Elementary Particle Physics, Cornell University, Ithaca, New York 14853, USA*

(Received 12 November 2003; published 22 April 2004)

Capitalizing on recent advances in lattice QCD, we present a calculation of the leptonic decay constants f_{B_s} and f_{D_s} that includes effects of one strange sea quark and two light sea quarks via an improved staggered action. By shedding the quenched approximation and the associated lattice scale uncertainty, lattice QCD greatly increases its predictive power. Nonrelativistic QCD is used to simulate heavy quarks with masses between $1.5m_c$ and m_b. We arrive at the following results: $f_{B_s} = 260 \pm 7 \pm 26 \pm 8 \pm 5$ and $f_{D_s} = 290 \pm 20 \pm 29 \pm 29 \pm 6$ MeV. The first quoted error is the statistical uncertainty, and the rest estimate the sizes of higher order terms neglected in this calculation. All of these uncertainties are systematically improvable by including another order in the weak coupling expansion, the nonrelativistic expansion, or the Symanzik improvement program.

DOI: 10.1103/PhysRevLett.92.162001 PACS numbers: 12.38.Gc, 13.20.Fc, 13.20.He

We present the first complete calculation of the B_s and D_s decay constants with three flavors of sea quarks with small masses. The D_s decay constant, f_{D_s}, has been measured [1,2], and the CLEO-c experiment promises to reduce the experimental errors significantly [3]. The comparison of experimental and lattice results will be a vital test of lattice QCD. The B_s and B_d decay constants, f_{B_s} and f_{B_d}, are necessary in order to constrain V_{td} via $\overline{B}^0 - B^0$ mixing. Since f_{B_s} will not be determined through direct measurement, an accurate lattice calculation is crucial for improving phenomenological tests of CKM unitarity.

The calculation presented below makes use of lattice Monte Carlo simulations, done by the MILC Collaboration [4], which include the proper sea quark content: one dynamical strange quark and two flavors of dynamical quarks with masses as light as $m_s/4$. The correct number of flavors is necessary in order for the lattice theory to have the same β function as real QCD. Only then can we expect, in principle, lattice results to agree with experimental measurements.

Inclusion of light up and down sea quarks is essential for accurate lattice phenomenology. The innovation which allows this on present computers is an improved staggered discretization of the light quark action [5–12]. The so-called "fourth-root trick" is used to simulate three-flavor QCD using a staggered fermion action. Despite some open theoretical issues concerning staggered fermion algorithms, results of improved staggered fermion calculations are free of ambiguities present in quenched simulations and agree very well with chiral perturbation theory, provided the u and d sea quark masses are light enough [13,14].

The removal of quenched artifacts permits a more precise study of systematic effects in lattice QCD simulations. Reference [12] presents lattice results for a variety of "gold-plated" quantities, those for which removal of lattice uncertainties is straightforward, such as f_π and f_K, and several splittings in the Υ spectrum. The change from $n_f = 0$ results, which differ substantially from experiment, to $n_f = 3$ results, which agree with experiment up to the 3% lattice uncertainties, suggests that gold-plated quantities can reliably be calculated with improved staggered fermion simulations. Heavy-light pseudoscalar leptonic decay constants fit into the gold-plated category.

Our calculation of f_{B_s} and f_{D_s} uses standard lattice QCD methods. Correlation functions were computed using a subset of gauge field configurations generated by the MILC Collaboration. The configurations include the effects of two dynamical light quarks with equal bare mass, denoted by $m_\ell^{\rm sea}$, and one dynamical strange quark, with bare mass $m_s^{\rm sea}$. The lattices we used have spacings of about 1/8 fm and volumes of about $(2.5\ {\rm fm})^3 \times 8.0$ fm. We focus on the configurations where $m_\ell^{\rm sea}/m_s^{\rm sea} = 1/5$ and 2/5. As we discuss below, the physical strange quark mass, m_s, obtained from the light hadron spectrum is actually 4/5 of $m_s^{\rm sea}$, so the light sea quark masses are approximately $m_s/4$ and $m_s/2$.

Details of the Monte Carlo simulations which generated the ensemble of gauge fields are given in [3]. In this Letter we use a level splitting in the Υ spectrum, e.g., the $\Upsilon(2S - 1S)$ splitting, to determine the lattice spacing, instead of the length scale r_1, derived from the static quark potential, which was used in [3]. The Υ spectrum will be presented in detail in a future publication [15]; however, we note here that as the light sea quark mass is increased, the $\Upsilon(1P - 1S)$ splitting becomes slightly smaller than experiment when the lattice spacing is set by $\Upsilon(2S - 1S)$. With statistical errors between 1%–2%,

the difference between experiment and lattice values for the $1P - 1S$ splitting is 0σ, 1σ, and 2σ for $m_\ell^{\rm sea}/m_s \approx 1/4$, $1/2$, and $3/4$, respectively. Except for estimating sea quark mass effects, we use the $m_\ell^{\rm sea}/m_s \approx 1/4$ lattice to obtain our results.

The analysis of [3] has also been updated with respect to determining the quark mass corresponding to the physical strange quark mass sector. Rather than using $\bar{s}s$ mesons which are either unstable (the ϕ) or do not exist (the pseudoscalar) we use the results of the partially quenched chiral perturbation theory analysis of m_K and m_π and take the bare value of m_s from fits to π and K masses and decay constants [13,14]. The result is that the $m_s^{\rm sea}$ is heavier than the physical strange quark mass by a factor of 5/4. The valence strange quark mass is set equal to the physical value.

A nonrelativistic action which is correct through $O(\Lambda_{\rm QCD}^2/m_Q^2)$ is used for the heavy quark, with coefficients set to their tree-level values. Table I lists the bare heavy quark masses used in this Letter, along with the corresponding nonrelativistic QCD (NRQCD) stabilization parameter n. For each mass, we estimate the heavy-light meson mass two ways: the "kinetic mass" $m_{H_s}^{\rm kin}$ is extracted from finite momentum correlators using the meson dispersion relation, and the "perturbative mass" $m_{H_s}^{\rm pert}$ is estimated from the zero momentum correlator and the one-loop heavy quark mass renormalization. We find that the bare heavy quark mass $aM_0 = 2.8$ produces the correct experimental mass for the Υ [16] and the B_s within statistical errors.

When we construct correlation functions for heavy-light mesons, we use the equivalence between staggered and naive fermion propagators. The operators we use are the same ones as with Wilson-like discretizations or in the continuum limit. This method for computing the B_s mass and decay constant has been presented, along with tests on quenched lattices, in recent work [17].

The B_s decay constant is defined through the axial vector matrix element; $\langle 0|A_\mu|B_s(p_\mu)\rangle = f_{B_s} p_\mu$. Here we use only the temporal component. Up through $O(1/M_0)$ three lattice operators contribute to A_0, the leading-order current, $J_0^{(0)} = \overline{q}\gamma_5\gamma_0 Q$, and two subleading currents $J_0^{(1)} = \overline{q}\gamma_5\gamma_0(\boldsymbol{\gamma}\cdot\boldsymbol{\nabla})Q/2M_0$ and $J_0^{(2)} = \overline{q}(\boldsymbol{\gamma}\cdot\boldsymbol{\overleftarrow{\nabla}})\ \gamma_5\gamma_0 Q/2M_0$; the matching from the lattice to the continuum is done in perturbation theory [18]. A one-loop calculation yields

$$A_0 = (1 + \alpha_s\tilde{\rho}_0)J_0^{(0)} + (1 + \alpha_s\rho_1)J_0^{(1,{\rm sub})} + \alpha_s\rho_2 J_0^{(2,{\rm sub})}, \tag{1}$$

where $J_0^{(1,{\rm sub})} = J_0^{(1)} - \alpha_s\zeta_{10}J_0^{(0)}$, and so too for $J_0^{(2,{\rm sub})}$. These operators explicitly subtract, through one loop, the power-law mixing of $J_0^{(0)}$ with $J_0^{(1)}$ and $J_0^{(2)}$ [19]. The perturbative calculation which determines $\tilde{\rho}_0$, ρ_1, ρ_2, ζ_{10}, and ζ_{20} will be presented separately [20].

From fits to correlation functions, we extract the combination $\Phi_{H_s} \equiv f_{H_s}\sqrt{m_{H_s}}$. Let us denote by $\Phi^{(i)}$ the contribution of $J_0^{(i)}$ to Φ_{H_s}. For this calculation the matrix elements are computed for mesons at rest, so $\Phi^{(1)} = \Phi^{(2)}$. Table II summarizes fits to the numerical data, converted to physical units using $1/a = 1.59(2)$ GeV for the $m_\ell^{\rm sea} \approx m_s/4$ lattice and $1/a = 1.61(2)$ GeV for the $m_\ell^{\rm sea} \approx m_s/2$ lattice. [The quoted uncertainties come from statistical and fitting uncertainties in the $\Upsilon(2S - 1S)$ splitting [15].] By comparing $\Phi^{(1)}/\Phi^{(0)}$ with $\Phi^{(1,{\rm sub})}/\Phi^{(0)}$ one can observe the sizable power-law mixing of $J^{(0)}$ with $J^{(1)}$. The expression (1) absorbs the mixing back into the term proportional to $J^{(0)}$, so $\Phi^{(1,{\rm sub})}/\Phi^{(0)}$ represents the physical contribution of $1/M_0$ terms to Φ_{H_s} up to two-loop corrections. The 4% contribution from the $1/M_0$ operator we see for the B_s ($aM_0 = 2.8$) is the same size seen in quenched studies over a range of lattice spacings [19].

Figure 1 shows the heavy quark mass dependence of Φ_{H_s} on m_{H_s} (plotted as squares). The data are fit well by

$$\Phi_{H_s} = \Phi_{H_s}^{\rm stat}\left(1 + \frac{C_1}{m_{H_s}} + \frac{C_2}{m_{H_s}^2}\right) \tag{2}$$

TABLE I. Heavy quark parameters and meson masses for two values of the light sea quark mass.

		$m_\ell^{\rm sea} \approx m_s/4$ (568 config)		$m_\ell^{\rm sea} \approx m_s/2$ (468 config)	
aM_0	n	$m_{H_s}^{\rm kin}$ (GeV)	$m_{H_s}^{\rm pert}$ (GeV)	$m_{H_s}^{\rm kin}$ (GeV)	$m_{H_s}^{\rm pert}$ (GeV)
2.8	2	5.6(2)	5.3(4)	5.22(17)	5.4(4)
2.1	4	4.38(10)	4.2(3)	4.28(11)	4.3(3)
1.6	4	3.52(6)	3.5(3)	3.56(7)	3.5(3)
1.2	6	2.84(5)	2.78(19)	2.93(4)	2.83(19)
1.0	6	2.53(4)	2.41(16)	2.60(3)	2.45(16)

TABLE II. Simulation results for $\Phi_{H_s} \equiv f_{H_s}\sqrt{m_{H_s}}$ for each light sea quark mass and heavy quark mass. The second column lists the leading order term $\Phi^{LO} \equiv (1 + \alpha_s\tilde{\rho}_0)\Phi^{(0)}$, The third and fourth columns show the contributions of $J_0^{(1)}$, with respect to $\Phi^{(0)}$, before and after the power law subtraction. The fifth column gives the result for Φ_{H_s}. Statistical and fitting uncertainties are quoted in parentheses (not including the statistical uncertainty in $1/a$).

$m_\ell^{\rm sea}/m_s \approx 1/4$				
aM_0	$\Phi^{LO}({\rm GeV}^{3/2})$	$\Phi^{(1)}/\Phi^{(0)}$	$\Phi^{(1,{\rm sub})}/\Phi^{(0)}$	$\Phi_{H_s}({\rm GeV}^{3/2})$
2.8	0.640(11)	−9.0(4) %	−3.7(4) %	0.614(13)
2.1	0.598(10)	−11.7(4) %	−5.0(4) %	0.565(11)
1.6	0.557(8)	−14.7(4) %	−6.4(4) %	0.516(9)
1.2	0.519(7)	−18.3(4) %	−7.8(4) %	0.470(8)
1.0	0.499(6)	−20.7(4) %	−8.6(4) %	0.445(7)
$m_\ell^{\rm sea}/m_s \approx 1/2$				
aM_0	$\Phi^{LO}({\rm GeV}^{3/2})$	$\Phi^{(1)}/\Phi^{(0)}$	$\Phi^{(1,{\rm sub})}/\Phi^{(0)}$	$\Phi_{H_s}({\rm GeV}^{3/2})$
2.8	0.640(15)	−8.9(6) %	−3.6(6) %	0.615(14)
2.1	0.599(11)	−11.4(6) %	−4.7(6) %	0.567(12)
1.6	0.563(7)	−14.2(5) %	−5.9(5) %	0.523(9)
1.2	0.528(6)	−17.7(5) %	−7.1(5) %	0.481(6)
1.0	0.510(6)	−20.0(5) %	−7.9(5) %	0.459(6)

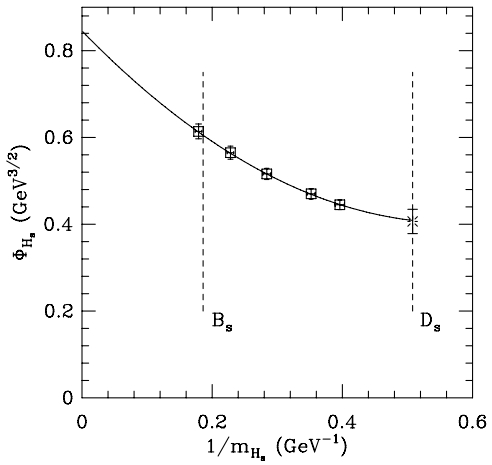

FIG. 1. Squares show $\Phi_{H_s} \equiv f_{H_s}\sqrt{m_{H_s}}$ vs $1/m_{H_s}$ on the $m_\ell^{\rm sea}/m_s \approx 1/4$ lattice. The solid line shows the fit described in the text, and the asterisk shows the value of Φ_{H_s} extrapolated to the charm sector. Experimental values for $1/m_{B_s}$ and $1/m_{D_s}$ are shown as dashed vertical lines.

with a correlated χ^2 per degree of freedom of 0.7/2. We find $\Phi_{H_s}^{\rm stat} = 0.85(4)$ GeV$^{3/2}$, $C_1 = -1.82(20)$ GeV, and $C_2 = 1.59(35)$ GeV^2. It is instructive to note that at $O(\Lambda_{\rm QCD}/m_Q)$ most of the mass dependence of Φ_{H_s} comes through the action and not through the currents. A fit to the leading-order $\Phi^{LO} \equiv (1 + \alpha_s\rho_0)\Phi^{(0)}$ (Table II) yields similar fit parameters: $\Phi^{{\rm stat},LO} = 0.83(4)$ GeV$^{3/2}$, $C_1^{LO} = -1.53(19)$ GeV, and $C_2^{LO} = 1.32(32)$ GeV^2. Since the action is accurate through $O(\Lambda_{\rm QCD}^2/m_Q^2)$, performing the operator matching through $O(1/M_0^2)$ should yield only small corrections to the values for $\Phi_{H_s}^{\rm stat}$, C_1 listed above. If the small effect of the $1/M_0$ currents can be taken as a guide, then including the $1/M_0^2$ currents should have a small effect on C_2.

We use the fit above to interpolate Φ_{H_s} slightly to the physical value of $1/m_{B_s}$. The result is $f_{B_s} = 260(7)$ MeV, where the quoted statistical error combines statistical errors from $1/a$ and $a^{3/2}\Phi_{B_s}$. Uncertainties in $m_{H_s}^{\rm kin}$ are small compared to the other uncertainties in the fit. The systematic uncertainties due to the neglect of higher order terms are estimated by assuming coefficients of $O(1)$. For example, two-loop terms omitted in (1) are estimated to be 10% effects, taking the coupling constant defined through the plaquette $\alpha_s = \alpha_P^{n_f=3}(2/a) = 0.32$ [21]. This is the largest systematic uncertainty. Leading discretization errors are $O(\alpha_s a^2\Lambda_{\rm QCD}^2)$, where $\Lambda_{\rm QCD}$ is the typical scale of nonperturbative dynamics. Taking $1/a = 1.6$ GeV and $\Lambda_{\rm QCD} = 400$ MeV implies 2% cutoff effects. The operator matching neglects terms $O(\Lambda_{\rm QCD}^2/m_b^2)$ or approximately 1%, and the NRQCD action neglects terms $O(\alpha_s\Lambda_{\rm QCD}/m_Q)$ which is about 3% for bottom quarks. Therefore, we quote an overall 3% uncertainty due to relativistic corrections.

Extrapolating the fit described above to the physical value for $1/m_{D_s}$ requires care since higher order terms in $1/m_{H_s}$ become increasingly important. The fit above extrapolates to $f_{D_s} = 290(10)$ MeV. We use a Bayesian analysis to estimate possible effects due to higher order terms. Allowing terms such as $C_n/m_{H_s}^n$ with $n \geq 3$ in the fit (2), with Gaussian priors for $C_n/{\rm GeV}^n = 0 \pm \delta$ and $\delta = 1 - 4$, we find higher order terms could lead to a 20 MeV error in f_{D_s}. This is taken as the statistical and fitting uncertainty. The $O(\alpha_s^2)$ perturbative error and the $O(\alpha_s a^2\Lambda_{\rm QCD}^2)$ discretization error are again estimated to be 10% and 2%, respectively. For charmed mesons $\Lambda_{\rm QCD}/m_c = 1/4$, so the $O(\Lambda_{\rm QCD}^2/m_Q^2)$ and $O(\alpha_s\Lambda_{\rm QCD}/m_Q)$ corrections to the matching are estimated to be 6% and 8%, respectively, so we quote a combined 10% estimate of possible relativistic corrections.

Figure 2 shows Φ_{H_s} vs light sea quark mass for two heavy quark masses, focusing on $m_\ell^{\rm sea} \leq m_s/2$. As $m_\ell^{\rm sea}$ decreases to the physical up/down masses, the $m_\ell^{\rm sea}$ dependence of Φ_{H_s} should be mild since no pion loops enter this quantity at leading order in heavy-light chiral perturbation theory. Within the uncertainties of the Υ splittings used to set the lattice spacing, no sea quark mass dependence is observed in Fig. 2. Consequently, the results for Φ_{H_s} computed with smaller values of $m_\ell^{\rm sea}$ would be consistent with the $m_\ell^{\rm sea} \approx m_s/4$ points, so we use these data points for the central values of f_{B_s} and f_{D_s}.

Experimental determination of the D_s leptonic decay constant is challenging, so this is a rare case where lattice QCD can lead experiment. The most recent and precise experimental results for f_{D_s} are $280 \pm 17 \pm 25 \pm 34$ MeV [1] and $285 \pm 19 \pm 40$ MeV [2], which agree well with the calculation presented here. Shrinking the experimental uncertainties on f_{D_s} is a major goal of the CLEO-c program.

Turning to comparison with the existing literature on lattice QCD, we quote recent world averages and comment on another new result. The $n_f = 3$ results presented here have central values larger than lattice calculations

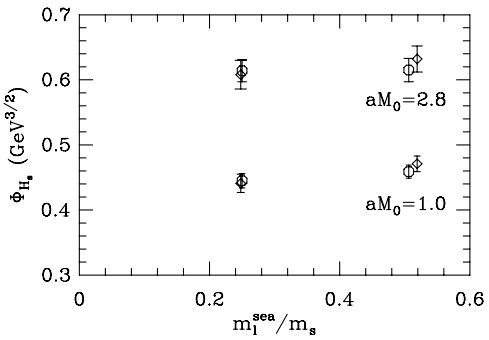

FIG. 2. Dependence of Φ_{H_s} on the light sea quark mass. The upper data points correspond to the B_s ($aM_0 = 2.8$) and the lower points come from our lightest heavy quark mass, $aM_0 = 1.0$. The different symbols indicate which quantity was used to set the lattice spacing: octagons use the $\Upsilon(2S - 1S)$ splitting and diamonds use the $\Upsilon(1P - 1S)$ splitting. Error bars represent combined statistical uncertainties of $1/a$ and $a^{3/2}\Phi_{H_s}$.

with $n_f = 0$ or 2. For example, recent averages [22] of quenched results are $f_{B_s}^{n_f=0} = 200(20)$ and $f_{D_s}^{n_f=0} = 230(14)$ MeV, significantly lower than our results. The two flavor world averages, $f_{B_s}^{n_f=2} = 230(30)$ and $f_{D_s}^{n_f=2} = 250(30)$ MeV, are higher than the quenched and agree within the quoted uncertainties.

Recently the JLQCD Collaboration reported a lattice QCD result using two dynamical flavors of improved Wilson fermions with mass between 0.7 and $2.9m_s$ [23]. They quote $f_{B_s} = 215(9)(^{+0}_{-2})(13)(^{+6}_{-0})$ MeV, with the first error statistical, second from chiral extrapolation of the sea quark mass, third from finite lattice spacing combined with truncation of NRQCD and perturbative expansions, and the fourth from ambiguity in setting the strange quark mass. This calculation uses much larger quark masses than ours, uses unstable hadron masses to set the lattice spacing and m_s, and does not include a dynamical strange quark. Each of these effects could cause a difference from our result. For example, CP-PACS found an approximate 15% difference in the latttice spacing determination between using m_ρ and the $1P - 1S$ Υ splitting [24]. Further work will be required to determine which combination of effects accounts for the difference with our result.

Recent sum rule calculations agree within errors for the B_s decay constant:, e.g., $f_{B_s}^{\text{s.r.}} = 236(30)$ MeV [25,26]. On the other hand, they do not calculate an increase in the decay constant as the heavy quark mass decreases:, e.g. $f_{D_s}^{\text{s.r.}} = 235(24)$ MeV [26].

To summarize, we have completed a calculation of the B_s and D_s decay constants using three-flavor lattice QCD. The more realistic sea quark content allows a unique lattice spacing to be determined using one of several quantities [13], enabling more reliable predictions. Our final results are

$$\begin{aligned} f_{B_s} &= 260 \pm 7 \pm 26 \pm 8 \pm 5 \text{ MeV}, \\ f_{D_s} &= 290 \pm 20 \pm 29 \pm 29 \pm 6 \text{ MeV}. \end{aligned} \tag{3}$$

The uncertainties quoted are, respectively, due to statistics and fitting, perturbation theory, relativistic corrections, and discretization effects. The result for the D_s decay constant agrees with experimental determinations, and the result for the B_s decay constant is a prediction. Improvement of the lattice results requires a two-loop perturbative matching calculation or the use of fully nonperturbative methods. On the other hand, much of the perturbative uncertainty cancels in the ratio f_{B_s}/f_{B_d}. Work is underway to study f_{B_d} using the methods discussed in this Letter [27].

Simulations were performed at NERSC. We thank the MILC Collaboration for their gauge field configurations. This work was supported in part by the DOE, NSF, PPARC, and the EU.

[1] CLEO Collaboration, M. Chadha *et al.*, Phys. Rev. D **58**, 032002 (1998).
[2] ALEPH Collaboration, A. Heister *et al.*, Phys. Lett. B **528**, 1 (2002).
[3] R. S. Galik, Nucl. Phys. (Proc. Suppl.) **B119**, 22 (2003).
[4] C.W. Bernard *et al.*, Phys. Rev. D **64**, 054506 (2001).
[5] C.W. Bernard *et al.*, Nucl. Phys. (Proc. Suppl.) **A60**, 297 (1998).
[6] G. P. Lepage, Nucl. Phys. (Proc. Suppl.) **A60**, 267 (1998).
[7] C.W. Bernard *et al.*, Phys. Rev. D **58**, 014503 (1998).
[8] G. P. Lepage, Phys. Rev. D **59**, 074502 (1999).
[9] K. Orginos and D. Toussaint, Phys. Rev. D **59**, 014501 (1999).
[10] D. Toussaint and K. Orginos, Nucl. Phys. (Proc. Suppl.) **73**, 909 (1999).
[11] K. Orginos, D. Toussaint, and R. L. Sugar, Phys. Rev. D **60**, 054503 (1999).
[12] C. Bernard *et al.*, Phys. Rev. D **61**, 111502 (2000).
[13] C. T. H. Davies *et al.*, Phys. Rev. Lett. **92**, 022001 (2004).
[14] C. Aubin *et al.*, hep-lat/0309088.
[15] A. Gray *et al.* (to be published).
[16] A. Gray *et al.*, Nucl. Phys. (Proc. Suppl.) **119**, 592 (2003).
[17] M. Wingate, J. Shigemitsu, C. T. H. Davies, G. P. Lepage, and H. D. Trottier, Phys. Rev. D **67**, 054505 (2003).
[18] C. J. Morningstar and J. Shigemitsu, Phys. Rev. D **57**, 6741 (1998).
[19] S. Collins, C. Davies, J. Hein, G. P. Lepage, C. J. Morningstar, J. Shigemitsu, and J. H. Sloan, Phys. Rev. D **63**, 034505 (2001).
[20] E. Gulez, J. Shigemitsu, and M. Wingate, Phys. Rev. D **69**, 074501 (2004).
[21] C. Davies *et al.*, hep-lat/0209122.
[22] S. M. Ryan, Nucl. Phys. (Proc. Suppl.) **106**, 86 (2002).
[23] JLQCD Collaboration, S. Aoki *et al.*, Phys. Rev. Lett. **91**, 212001 (2003).
[24] A. Ali Khan *et al.*, Phys. Rev. D **64**, 054504 (2001).
[25] M. Jamin and B. O. Lange, Phys. Rev. D **65**, 056005 (2002).
[26] S. Narison, Phys. Lett. B **520**, 115 (2001).
[27] M. Wingate *et al.*, hep-lat/0309092.